Materials Transactions, Vol. 44, No. 2 (2003) pp. 239 to 246

Change in Vickers Hardness and Substructure during Creep of a Mod.9Cr–1Mo Steel*

Takao Endo[1], Fujimitsu Masuyama[2] and Kyu-Seop Park[1]

[1]*Department of Materials Engineering, Yokohama National University, Yokohama 240-8501, Japan*
[2]*Nagasaki Research & Development Center, Mitsubishi Heavy Industries, Ltd., Nagasaki 851-0392, Japan*

In order to investigate the structural degradation during creep, interrupted creep tests were conducted of a Mod.9Cr–1Mo steel in the range of stress and temperature from 71 to 167 MPa and 873 to 923 K. The change of hardness and tempered martensitic lath width were measured in grip and gauge parts of interrupted specimens. The lath structure was thermally stable in static conditions, however, it was not stable during creep and the structural change was enhanced by creep strain. The relation between the change in lath width and strain was described quantitatively. The change in Vickers hardness was expressed by a single valued function of creep life consumption ratio. Based on the empirical relation between strain and lath width, a model was proposed to describe the relation between change in hardness and creep life consumption ratio. The comparison of the model with the empirical relation suggests that about 65% of hardness loss is due to the decrease of dislocation density accompanied by the movement of lath boundaries. The role of precipitates on subboundaries was discussed in connection with the abnormal subgrain growth appearing in low stress regime.

(Received September 2, 2002; Accepted December 13, 2002)

Keywords: *creep, creep life, life assessment, lath width, hardness, subgrain*

1. Introduction

The modification of conventional 9Cr–1Mo steel (T9) has led to the standardization of T91 (modified 9Cr–1Mo steel) in the USA in 1983.[1,2] Because of its superiority in terms of high temperature strength and small thermal expansion coefficient, it has been exploited in Japan since 1985, and the amount used is increasing in power plants. As a results, long-term service aged components are now growing, and the elaboration of life assessment technology is demanded for this material.

In order to meet the requirements for creep life assessment, studies on the constitutive equations,[3–6] the substructural evolution,[7–9] the growth of precipitates during creep,[10] and also the relation between creep strength and structures[11–15] have been investigated. Among these works, the observation reported by Kushima *et al.*[14] is worthy of attention. They found that the decrease in creep life and rupture strain, which emerged when creep life exceeded 10000 h, was associated with abnormal subgrain growth occurring in the vicinity of prior austenite grain boundaries. To investigate this phenomenon more closely, Suzuki *et al.*[15] studied the precipitates near prior austenite grain boundaries, and found Z phase particles growing rapidly at the sacrifice of fine MX particles containing Nb and V. Based on their observations, they ascribed the abnormal subgrain growth to the Z phase particles appearing preferentially near prior austenite grain boundaries.

Their new finding is quite important in understanding the loss of creep strength in long term creep. However, the structural evolution in short term creep is also important to deepen the understanding of structural degradation. In the present paper, the change of hardness and tempered martensitic lath width, and also the relation among hardness, creep life and lath width will be treated quantitatively, followed by discussion on the structural evolution and the non-homogeneous recovery of lath structure appearing in low stress regimes.

2. Experimental Procedure

The heat treatment applied an as-received Mod.9Cr–1Mo steel (ASME SA-213 T-91) was normalization at 1313 K for 1 h and tempering at 1053 K for 2 h. The chemical compositions of the material are shown in Table 1. Two series of interrupted creep tests, A and B, were conducted at atmospheric pressure. Creep specimens with two shoulders in both ends had a gauge part of 30 mm in length and 6 mm in diameter. The stress and temperature for series A were 157 to 186 MPa and 873 to 898 K, respectively and those for series B were 71 to 115 MPa and 873 to 923 K, respectively. In series A tests, strain-time relations were automatically recorded. The measurements of ambient hardness and TEM observation were carried out on the gauge and grip parts of interrupted specimens. The load applied for the Vickers hardness measurements was 2 kg for 30 s. The initial hardness (H_0) was 225 and 214 for series A and B, respectively.[16] In series B tests, only the hardness measurements were conducted, and the creep curve was not recorded. The longest creep life of series A was 1185 h and that of series B was 18736 h.

Table 1 Chemical Composition in mass%.

C	Si	Mn	P	S	Ni
0.1	0.25	0.4	0.016	0.005	0.04
Cr	Mo	Nb	Al	V	N
8.4	0.9	0.07	0.005	0.21	0.044

*This Paper was Originally Published in Japanese in *Tetsu-to-Hagané* **88** (2002) 526–533.

3. Experimental Results

3.1 Change in Vickers Hardness due to creep

Examples of interrupted and uninterrupted creep curves are shown in Fig. 1 in which interrupted time and strain are given. These creep curves are characterized by a relatively long primary creep common to tempered martensitic structure steels.[3] The measurements of Vickers hardness were carried out on the grip and gauge parts of crept specimens. For the convenience of description, the change in hardness ratio (H/H_0) from 657 to 18736 h and that of 22.4 to 1185 h are shown separately as a function of time in Figs. 2 and 3, respectively. The decrease in hardness ratio can be expressed approximately by a linear relation of time, although the slope of the lines depends on creep conditions. It should be noted that the decrease of hardness is much smaller in the grip parts than in the gauge parts. This clearly demonstrates that the as-received structures are thermally stable if strain is not applied to the material.[6]

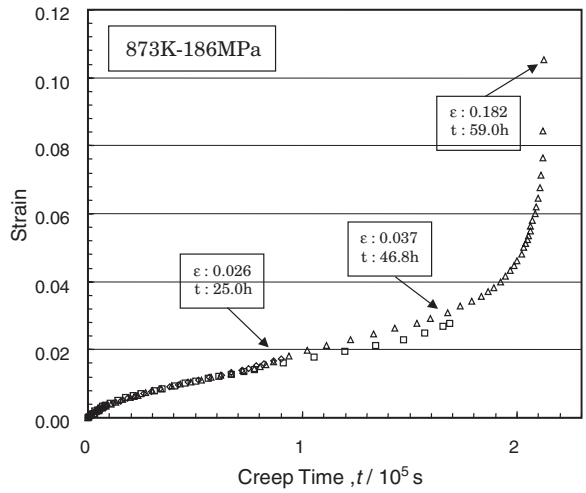

Fig. 1 An example of interrupted and uninterrupted creep curves tested at 186 MPa and 873 K.

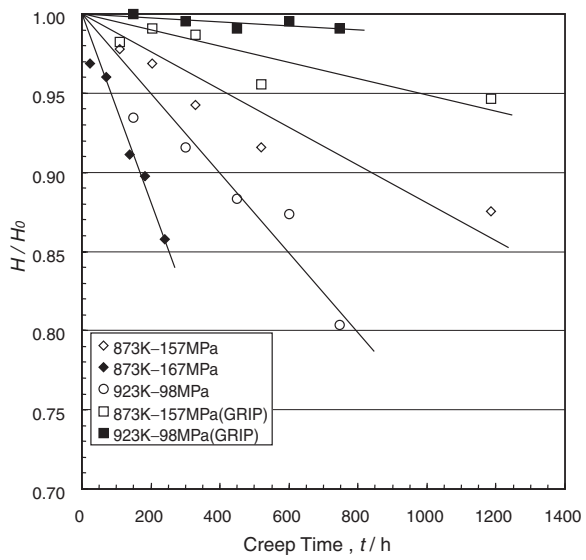

Fig. 2 Change in Vickers hardness ratio (H/H_0) with creep time for the interrupted specimens whose interruption time is from 657 to 18736 h, where H_0 and H are the ambient hardness before and after creep interruption, respectively.

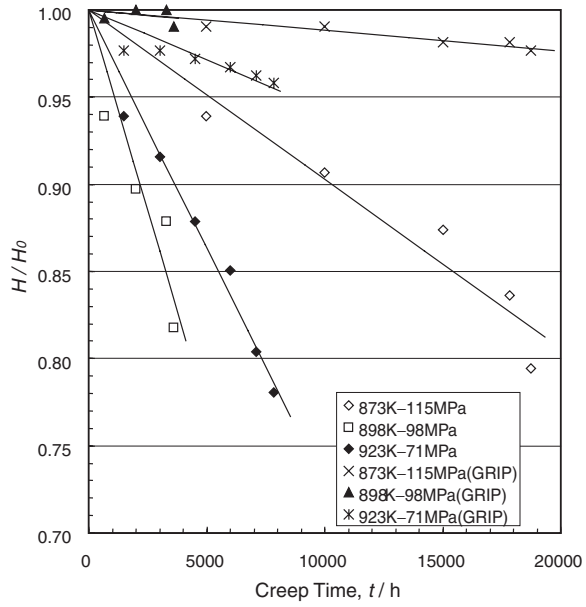

Fig. 3 Change in Vickers hardness ratio (H/H_0) with creep time for the interrupted specimens whose interruption time is from 22.4 to 1185 h.

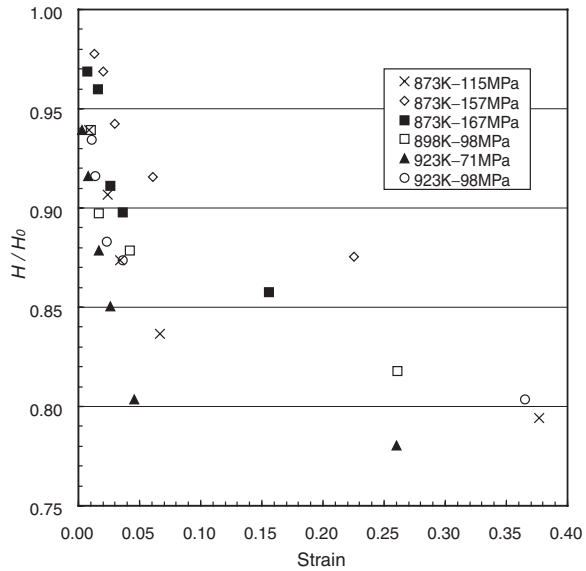

Fig. 4 Relation between the change in hardness ratio and creep strain.

The relation between hardness change and strain is depicted in Fig. 4. The figure shows that the change in hardness is greater in the case of smaller strains. The relation between hardness ratio and life consumption ratio (LCR), normalized time divided by the corresponding creep life, is shown in Fig. 5. Although there is some scattering as LCR approaches unity, the hardness ratio can be expressed as a function of LCR as bellow;

$$H/H_0 = 1 - 0.19(t/t_r) \quad (1)$$

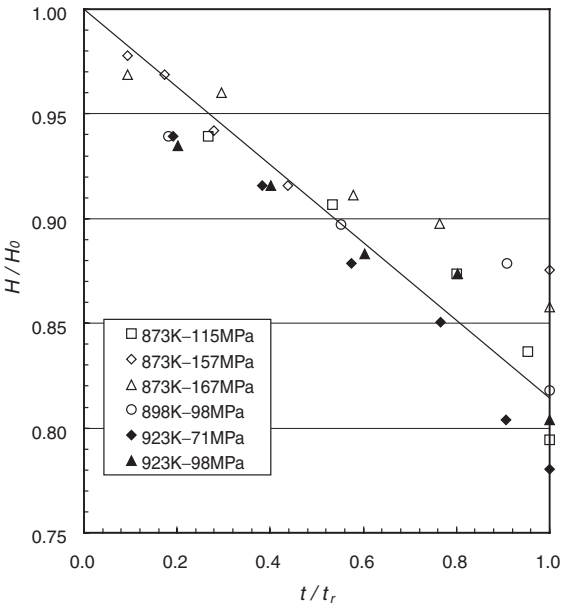

Fig. 5 Relation between hardness ratio and life consumption ratio (t/t_r), normalized time divided by the corresponding creep life, t_r.

3.2 Lath structures of interrupted specimens

As described in the previous section, Vickers hardness in the gauge parts decreases with increase in LCR. Structural observation was carried out by TEM on interrupted creep specimens. Figure 6(a) shows the microstructure of an as-received specimen. The micrograph shows a randomly oriented lath structure, and the lath width of an as-received specimen was about 0.54 µm. There remain the densely populated dislocations within lath boundaries introduced in martensitic transformation, and many carbides are also seen along prior austenite, packet, block or lath boundaries. Their shape and size suggest that carbides are mostly of $M_{23}C_6$ type.

Figures 6(b) to (d) show the microstructures of the gauge parts tested at 873 K and 167 MPa. The interrupted creep strains are given in these figures. It is to be noted that the lath width increases continuously with increasing creep strain, and the shape of the lath structure changes gradually from an initial rectangular shape to a round one. As Sawada *et al.*[15] showed, dislocation density within lath boundaries decreases gradually as the creep strain increases. In some cases we could not identify the lath boundary even if the precipitates lined up clearly. These lined-up precipitates indicate the position where the lath boundary was located before creep.

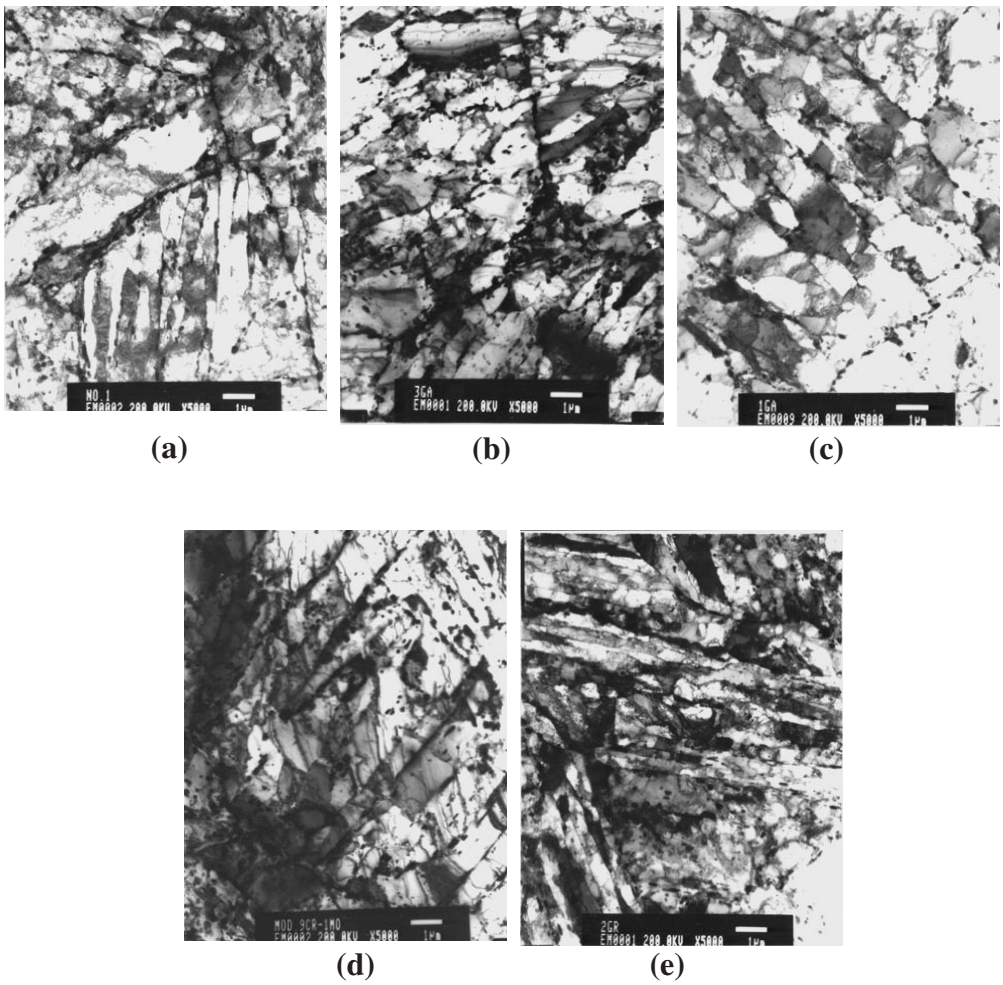

Fig. 6 TEM micrograph showing the change of tempered martensitic structures with creep strain. Testing stress and temperature are 167 MPa and 873 K, respectivly. (a) as-received, lath width (w) = 0.54 µm (b) $\varepsilon = 5.5\%$, and $w = 0.74$ µm, (c) $\varepsilon = 8.2\%$, and $w = 0.90$ µm, (d) $\varepsilon = 15.6\%$, and $w = 0.99$ µm, (e) substructures of a grip part after creep rupture.

Figure 6(e) shows the substructures of the grip part, which are similar to those of the as-received specimens and dissimilar to those of the gauge parts. Actually, the lath width of grip parts after rupture was about 0.55 μm which was close to the initial lath width. This fact corresponds to the smaller change in hardness in the grip parts, and supports the speculation that the decrease in hardness of the gauge section is due to the decrease of the dislocation density caused by the migration of the lath boundaries.

3.3 Change in lath width with creep deformation

Since the lath width increases with strain, the measurements of lath width were carried out. The lath was rectangular in an initial state but changed to an equi-axed round one in the late stage of creep. In the present study, the distance between the shorter sides of a rectangle was taken as the lath width, and the diameter was taken for the round subgrains. The results of measured lath width are plotted against strain along with the results reported by other investigators[9,13,15] in Fig. 7. It is clear that the lath width increases with strain and the rate of increase in lath width, $dW/d\varepsilon$ becomes small as strain approaches rupture strain. It is necessary to emphasize here that creep rupture is generally associated with a local necking. In such a case, the nominal rupture strain is usually much larger than the true strain subjected to a foil sample for TEM study since the foil is taken from the gauge section well apart from the necking region. This is probably one of the reason why $dW/d\varepsilon$ becomes smaller as strain approaches that of creep rupture. From this standpoint, the lath width is plotted against strain in Fig. 8 omitting the data near rapture strain. Close examination of Fig. 8 suggests that the relationship between lath width and strain is expressed by a curve which is convex upward. Notwithstanding the above general trend, a relationship between them will be approximated by a straight line expressed in the form of eq. (2) for the sake of simplicity. As Fig. 8 shows, the slope of the lines depends on the stress when compared at about the same temperature.

$$\Delta W = \beta\varepsilon, \tag{2}$$

where β is the slope of the lines.

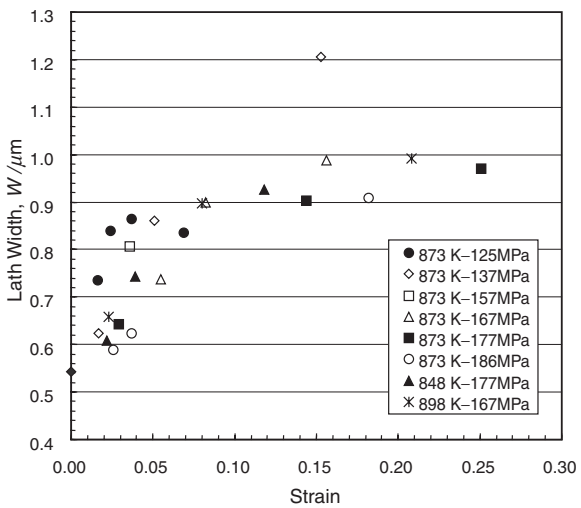

Fig. 7 Lath width as a function of creep strain.

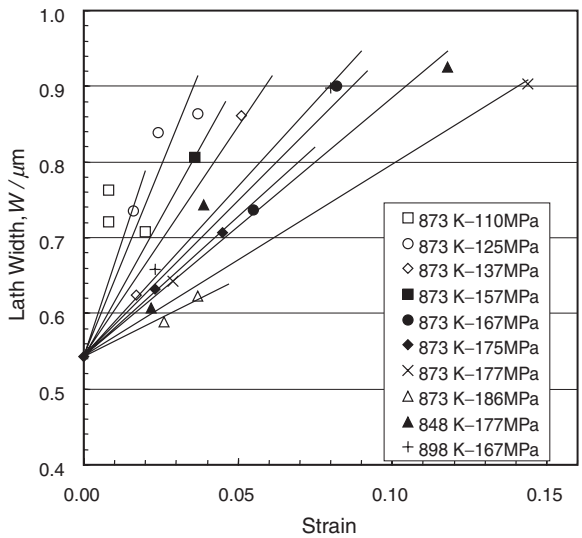

Fig. 8 Plot of lath width against creep strain by omitting the data near rapture strain.

4. Discussion

4.1 Stress and strain dependence of lath width

It is clear that the slope of the lines in Fig. 8 depends on stress. However, taking into account that the lath width approaches a constant value depending solely on stress, it is rather natural that the slope of the line depends on stress, since the lath width approaches a smaller value at higher stresses. Therefore, the values of ΔW divided by $(W_S - W_0)$ are shown as a function of strain in Fig. 9, where W_0 is the initial lath width,[17] and W_S is the final lath width depending solely on stress.[18] There is some scattering in plots, but all data points lay around a single line with the slope independent of stress and temperature. From this figure, ΔW can be expressed as below;

$$\Delta W = \alpha(W_S - W_0) \cdot \varepsilon, \tag{3}$$

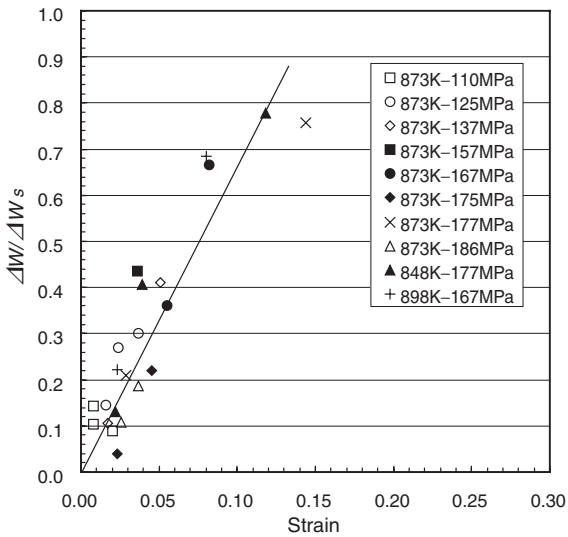

Fig. 9 Relation between ΔW divided by $(W_S - W_0)$ and creep strain, where W_0 is the initial lath width, and W_S is the final lath width depending solely on stress.

where α is the constant of the magnitude of about 6.7 μm.

4.2 Evolution of lath structure

As mentioned above, the structural observation in the grip parts shows that the lath structure does not evolve substantially. This suggests that the subboundaries are pinned with precipitates, and they cannot move easily without the influence of creep strain. However, once they escape from precipitates with the aid of stress and temperature, they can move and evolve readily making use of interfacial energy as a driving force for subgrain growth. Therefore, the growth process of lath structure will be treated in analogy with the grain growth[19] associated with the decrease of total interfacial energy.[20]

$$dW/dt = k\Gamma(1/W - 1/W_S), \tag{4}$$

where k is the proportional constant. When W_S is close to W_0, eq. (4) can be rewritten as,

$$dW/dt = k\Gamma(1/W_S - 1/W_0)/(W_S \cdot W_0). \tag{5}$$

Since the lath boundary is composed of dislocations introduced in martensitic transformation, the energy for lath boundary can be expressed in the form of a small angle boundary[21] as below:

$$\Gamma \cong A\theta(\ln B - \ln\theta) \cong A \cdot \theta \cong Ab/h, \tag{6}$$

where θ is the tilt angle of the boundary, A and B are constants, h is the separation between dislocations in the subboundaries, and b is the strength of Burgers vector. As eq. (6) shows, the interfacial energy Γ is proportional to the spacing between dislocations, h. Therefore, interfacial energy is expected to increase as the number of dislocations entering into lath boundaries increases.

Hereafter, densely populated dislocations within lath structures shall be classified into three categories, (1) a dislocation group which is bounded weakly by other dislocations or precipitates, (2) a dislocation group bounded moderately, and (3) a dislocation group bounded strongly with other dislocations and precipitates. Dislocations in the first category are expected to move relatively easily in the early stage of creep, and they contribute to the large primary creep common to tempered martensite structure materials.[22] Dislocations in the second category begin to move following the dislocations in the first category. Since they can travel a relatively large distance, they contribute to creep strain and the increase of lath boundary energy by entering into the subboundaries. As speculated above, the dislocation motion is quite complicated, however, dislocations in the second category will be considered for the sake of simplicity.

The dislocations in the second category are probably generated from tangled dislocations. So the dislocation density in the second category is expected to be proportional to the generation rate of dislocations released from dislocation tangles ($\dot{\rho}$). On the other hand, since the strain rate is proportional to $\dot{\rho}$, the lath boundary energy can be replaced by the strain rate. Taking this into consideration, eq. (5) can be rewritten as;

$$dW/dt = k'\dot{\varepsilon}(W_S - W_0), \tag{7}$$

where, k' is a constant. From eq. (7) following equation is obtained;

$$\Delta W = k'(W_S - W_0)\varepsilon. \tag{8}$$

It is to be noted that eq. (8) is similar to eq. (3).

In the deduction of eq. (8), we assumed that the W is close to W_0. However, eq. (8) holds even if the magnitude of W is twice as larger as that of W_0. This is probably because the interfacial energy is not constant all the way to rupture, but it is expected to increase in the late stage of creep because of increased dislocations entering into lath boundaries.

4.3 Relation between hardness and LCR

As-received tempered martensitic structure steels have high dislocation density, however, the dislocation density decreases during creep, and leads to structural degradation. At the present time, it is not clear what kind of mechanisms are operating in dislocation annihilation. In this section, an attempt will be made to explain the hardness loss in connection with the migration of subboundaries.

Let us supposed that lath boundaries migrate by ΔW during creep and that they absorb all the dislocations behind them. In this case, the average dislocation density (ρ) can be expressed as below;

$$\rho = \rho_0(W_0/W)^2, \tag{9}$$

where ρ_0 is the initial dislocation density.

Since the hardness at ambient temperature is expected to be proportional to the square root of dislocation density, eq. (10) results from eqs. (3) and (9) as;

$$\begin{aligned} H - H_0 &= [(W_0 - W)/W]H_0 \\ &= -[(W_S - W_0)/W] \cdot 6.7\varepsilon \cdot H_0. \end{aligned} \tag{10}$$

In order to relate eq. (10) with the empirical eq. (1), an attempt will be made to relate LCR with creep strain. Figure 10 shows the relation between the logarithm of the strain rate and true strain corresponding to Fig. 1. It is clear that the logarithm of the strain rate changes linearly with true strain over a relatively wide range. Therefore, the following equation[23–25] holds.

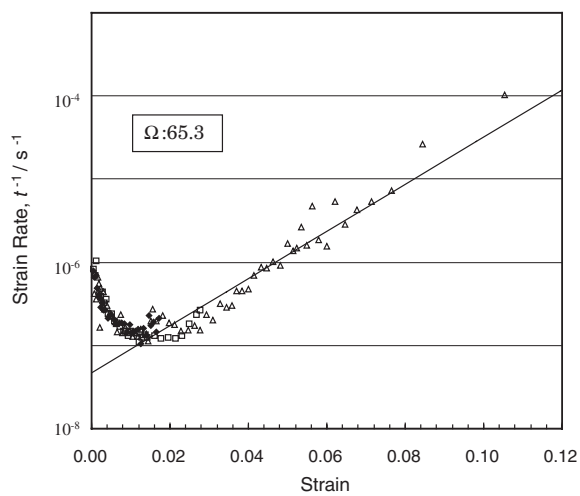

Fig. 10 Relation between logarithm of strain rate and true strain corresponding to Fig. 1.

$$\ln \dot{\varepsilon} = \ln \dot{\varepsilon}_0 + \Omega\varepsilon, \tag{11}$$

where ε is the instantaneous strain rate, $\dot{\varepsilon}_0$ is the imaginary initial strain rate, and Ω is the slope of the line (strain rate acceleration factor). Assuming that eq. (11) holds over an entire range of creep, creep life is expressed by eq. (12).[24,25] One can obtain creep strain by integrating eq. (11) with respect of time and making use of eq. (12).

$$t_r = 1/(\Omega\dot{\varepsilon}_0). \tag{12}$$

$$\varepsilon = (1/\Omega)\ln[1/(1 - t/t_r)]. \tag{13}$$

Equation (13) can be rewritten in the form;

$$\varepsilon \cong \psi(1/\Omega) \cdot (t/t_r), \tag{14}$$

where ψ is given by eq. (15).

$$\psi = \ln[1/(1 - t/t_r)]/t/t_r. \tag{15}$$

Comparison of eqs. (14) and (15) shows that the magnitude of ψ is unity at $t = 0$, and it increases up to about 7.

Using eq. (14), eq. (10) is rewritten in the form as:

$$H/H_0 = 1 - 6.7[(1/\Omega)\{(W_S - W_0)/W\}\psi](t/t_r). \tag{16}$$

Figure 11 shows the relation between the magnitude within the brackets of eq. (16) and LCR. The magnitude of Ω depends on stress and slightly on temperature,[3] however, its magnitude is about 64 in the present case. There is some scattering, however, the magnitude within the brackets of eq. (16) is a constant of about 0.02, so that the magnitude of the term in front of t/t_r in eq. (16) is about 0.13 which is about 65% of 0.19 in eq. (1). This means that about 65% of dislocations within lath structures are absorbed and eliminated by the movement of lath boundaries, and the rest of the dislocations are annihilated by other mechanisms such as mutual annihilation due to the motion of isolated and moderately bounded dislocations.

4.4 Non-homogenious recovery of lath structures

When creep duration exceeds 10000 h, creep life becomes shorter than that extrapolated from the short time creep data, and that rupture strain also becomes smaller.[15,26,27] Since the recent study[15] showed that this phenomenon had something to do with the non-homogeneous recovery of lath structures and the appearance of the Z phase, we will discuss this phenomena in connection with the knowledge obtained in the present study.

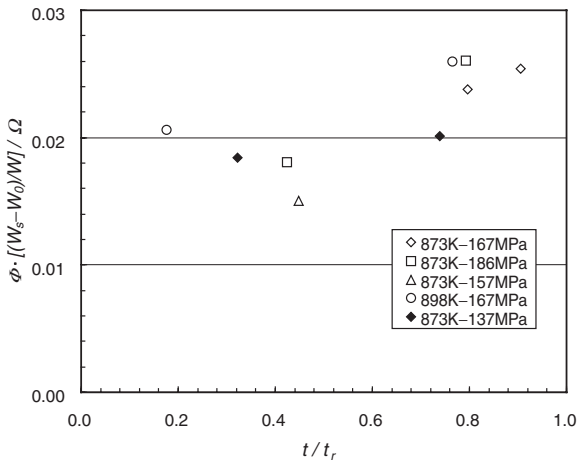

Fig. 11 Relation between the magnitude within the brackets of eq. (16) and LCR, (t/t_r).

As-received Mod.9Cr–1Mo steel exhibits tempered martensitic structures containing prior austenite, packet, block and lath boundaries. Their boundaries are decorated by carbides such as $M_{23}C_6$ and MX that appeared in the tempering process. This is the reason why the substructure is thermally stable in the grip parts. However, lath boundaries can move relatively easily under the influence of stress, and as a result, the dislocation density and hardness decrease readily in accordance with the lath boundary movement. In other words, subboundaries are supposed to be released from the pinning of carbides in the early stage of creep under the action of stress. Hereafter, stress needed for a sub boundary to unlock the pinning of carbides will be discussed.

Since the lath boundaries are composed of a group of dislocations which is introduced to relax the stress due to martensitic transformation, they can glide under the action of stress at elevated temperatures. Actually, there are some reports demonstrating the subboundary migration and its contribution to total creep strain.[28–33]

Let us suppose the subboundary along which precipitates of the size R are arranged at the intervals of Λ. Since the work necessary to move the subboundary by a distance $R/2$ is equal to the increase in interfacial energy due to the escape from precipitates on the boundary,[34,35] the stress required to detach the subboundary from precipitates is as follows;

$$\tau = \pi\Gamma Rh/\Lambda^2 b, \tag{17}$$

where h is the separation between dislocations composed of subboudaries, and Γ is the interfacial energy of lath boundary. On the other hand, Γ is expected to be of the form, $\Gamma = \alpha Gb^2/h$. Accordingly, the tensile stress needed to release a subboundary from the constraint of the precipitates is as below;

$$\sigma = \alpha M\pi GbR/\Lambda^2, \tag{18}$$

where M is the Taylor factor, G is the shear modulus, b is the Burgers vector, and α is the constant of the magnitude of about 0.5. Suzuki *et al.*[15] observed the precipitates along lath boundaries by filtered electron microscopy and showed that the magnitudes of Λ and R are about 500 nm and 50 to 2000 nm, respectively. Taking the values of G (= 6245 MPa), b (= 24.8 nm), α (= 0.5), M (= 2.0), and Λ = 500 nm and R = 1000 nm, the maginitude of σ was estimated crudely to be 100 MPa. The stress level in the present study is more than 100 MPa so that the assumption that the subboundary is free from the locking of precipitates appears reasonable. In contrast to the present study, Suzuki *et al.*[15] found the abnormal recovery of lath structure occurred at a stress less than 100 MPa. Therefore, the observation by Suzuki *et al.*[15] seems to correspond to the case where subboundaries cannot escape from the pinning of precipitates unless the carbides grow gradually and their carbide spacing increases.

Figure 12 shows the normalized subgrain size (W/b) at $t/t_r = 1$ plotted against normalized stress (σ/G). Except for

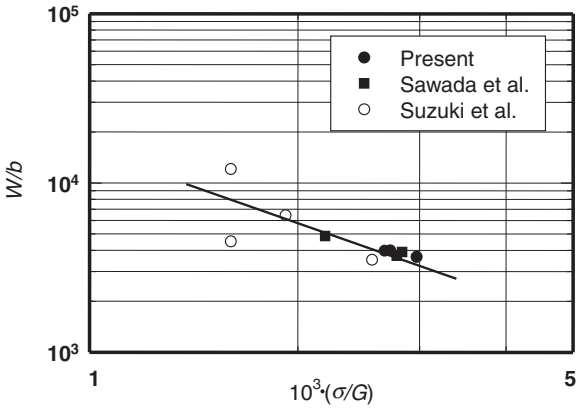

Fig. 12 Relation between normalized subgrain size (W/b) at $t/t_r = 1$ and normalized stress (σ/G).

the data at the lowest stress, almost all the data points fall around a single line expressed in the form $(W/b) = m(G/\sigma)$, where m is 16.3.[36] In the case of single phase materials, an analysis of many sets of data shows the similar relation with a constant of about 20.[37] This means that the average subgrain size of a Mod.9Cr–1Mo steel is close to that of single phase materials when crept to rupture at a stress above 137 MPa ($\sigma/G = 2.19 \times 10^{-3}$). In contrast to data points obtained above 137 MPa, the subgrain size obtained at 100 MPa is somewhat different in behavior. Actually, Suzuki *et al.*[15] pointed out that the relation between the area fraction and subgrain size exhibited a normal distribution above 100 MPa, however, it changed to the distribution with two peaks, at 7 μm^2 and 1 μm^2 at 100 MPa. This is because only some fraction of the subgrains exhibited an abnormal subgrain growth at 100 MPa. In fact, the smaller grain size at 100 MPa is much smaller than that expected from the data above 120 MPa. This fact demonstrates that most of subgrains failed to attain the final subgrain size even at $t/t_r = 1$. In other words, this fact claims that the most of the subgrain boundaries failed to escape from the pinning of precipitates at 100 MPa. Further studies are required on the relation among Z phase appearing at low stresses, abnormal subgrain growth, and Ostwald ripening of carbides during creep.

5. Summary

Aiming at the understanding of structural degradation during creep, interrupted creep tests, measurements of Vickers hardness and TEM observation have been carried out on a Mod.9Cr–1Mo steel at 873 to 923 K and 71 to 167 MPa. Results obtained in the present study are as follows;

(1) The structure of a Mod.9Cr–1Mo steel was thermally stable in static aging, however, the structural degradation was accelerated by creep strain.
(2) The change in Vickers hardness was expressed as a function of creep life consumption ratio in the form of eq. (1) in the text.
(3) The change of tempered lath width was approximately expressed as a function of creep strain in the form of eq. (3).
(4) The increase of lath width with creep strain was explained in analogy with the theory of grain growth driven by the change of interfacial energy.
(5) A model describing the relation between hardness and creep life consumption ratio was proposed. The model suggests that about 65% of hardness loss is due to the decrease of dislocation density accompanied by the movement of lath boundaries.
(6) The role of carbides along lath boundaries was discussed in connection with normal and abnormal subgrain growth during creep.

Acknowledgements

The authors would like to thank Mr. H. Nishino for his invaluable cooperation and help in carrying out the experiments. They would also like to thank the financial support from the Grant-in Aid for Science Research of the Ministry of Education, Culture, Sports, Science and Technology, Japan.

REFERENCES

1) ASTM A213-83.
2) ASME Boiler and Pressure Vessel Code, Case 1934. Seamless Modified 9Cr–1Mo Section I.
3) K. S. Park, F. Masuyama and T. Endo: *Tetsu-to Hagané* **84** (1998) 526–533.
4) K. S. Park, F. Masuyama and T. Endo: *Tetsu-to Hagané* **85** (1999) 492–499.
5) K. S. Park, F. Masuyama and T. Endo: ISIJ Int. **41** (2001) S86–90.
6) K. S. Park, F. Masuyama and T. Endo: J. Japan Inst. Metals **63** (1999) 597–600.
7) K. Sawada, K. Maruyama, R. Komine and Y. Nagae: *Tetsu-to-Hagané* **83** (1997) 466–471.
8) K. Sawada, M. Takeda, K. Maruyama, R. Komine and Y. Nagae: *Tetsu-to-Hagané* **84** (1998) 580–585.
9) K. Sawada, K. Maruyama, Y. Hasegawa and T. Muraki: *Creep and Fracture of Engineering Materials and Structures*, Ed. by T. Sakuma and K. Yagi, (Trans Tech Publications, Swiss, 1999) pp. 109–114.
10) E. Cerri, E. Evangelista, S. Spigarelli and P. Bianchi: Mater. Sci. Eng. **A245** (1998) 285–292.
11) K. Hamada, K. Tokuno and T. Takeda: Nucl. Eng. Des. **139** (1993) 277–281.
12) F. Masuyama and N. Nishimura: *Strength of Materials*, Ed. by H. Oikawa, K. Maruyama, S. Takeuchi and M. Yamaguchi, (JIM, 1994) pp. 657–660.
13) A. Orlova, J. Bursik, K. Kucharova and V. Sklenicka: Mater. Sci. Eng. **A245** (1998) 39–48.
14) H. Kushima, K. Kimura and F. Abe: *Tetsu-to Hagané* **85** (1999) 841–847.
15) K. Suzuki, S. Kumai, H. Kushima, K. Kimura and F. Abe: *Tetsu-to Hagané* **86** (2000) 550–557.
16) The measurements of hardness for series B were conducted by an ultrasonic hardness tester.
17) The initial lath width of the present work is 0.54 μm, and those of Sawada *et al.*,[9] Orlova *et al.*[13] and Suzuki *et al.*[15] are 0.6, 0.53 and 0.3 μm, respectively.
18) The final lath or subgrain size corresponding to rupture strains was estimated by an empirical relation shown in Section 5.
19) M. Hillert: Acta Metall. **13** (1965) 227–238.
20) Boundary energy and highly populated dislocations are the candidates of the driving force for structural evolution. As will be discussed in Section 4.3, the relation between dislocation density and the displacement of lath boundary can be expressed by eq. (9) when dislocations are absorbed by moving lath boundaries, and some of the dislocations annihilate in lath boundaries. In this case, $3\Gamma \geqq Gb^2W\rho$, is a criterion of whether the boundary energy is dominant or not in structural evolution. Substituting the appropriate values into the criterion, the lath boundary energy was found to be more important than strain energy of dislocations as the driving force for the present case.

21) W. T. Read, Jr.: *Dislocations in Crystls*, NewYork, (McGraw-Hill,1953) pp. 155–172.
22) Primary creep of a Mod.9Cr–1Mo steel was described by an equation of logarithmic creep.[4] Since the logarithmic creep can be well explained by the consumption theory of dislocations, the above fact is favorable to the hypothesis that the isolate dislocations of the first category contribute to the large primary creep of tempered martensitic steels.
23) R. Sandstrom and A. Konyr: ICM3, Cambridge, UK, 2 (1972) 275–284.
24) T. Endo and J. Shi: *Strength of Materials*, Ed. by H. Oikawa, K. Maruyama, S. Takeuchi and M. Yamaguchi, (JIM, 1994) pp. 665–668.
25) M. Prager: *Strength of Materials*, Ed. by H. Oikawa, K. Maruyama, S. Takeuchi and M. Yamaguchi, (JIM, 1994) pp. 571–574.
26) C. R. Brinkman, D. J. Alexander and P. J. Maziasz: Presented at the Jt.ASME/IEEE Power Generation Conference, ASME, New York. (1990).
27) Kouon Henkei Tokusei Deta Shyu, (ISIJ, Tokyo, 1992) 117–161.
28) S. F. Excell and D. H. Warrington: Philos. Mag. **26** (1972) 1121–1136.
29) H. Fukutomi and R. Horiuchi: J. Japan Inst. Metals **43** (1979) 1025–1031.
30) H. Fukutomi and R. Horiuchi: J. Japan Inst. Metals **45** (1981) 574–580.
31) M. Biberger and W. Blum: Philos. Mag. **A 65** (1992) 757–770.
32) M. Biberger and W. Blum: Philos. Mag. **A 66** (1992) 27–40.
33) W. Mueller, M. Biberger and W. Blum: Philos. Mag. **A 66** (1992) 717–728.
34) C. S. Smith: Quoted from H. G. Gleiter in *Physical Metallurgy*, Ed. By R. W. Cahn and P. Haasen (North-Holland Physics Publishing, Amsterdam-Oxford-New York-Tokyo, 1983) pp. 649–712.
35) T. Nishizawa, I. Ohmura and K. Ishida: Mater. Trans., JIM **38** (1977) 950–956.
36) The magnitude of G at a temperature from 823 to 923 K was estimated by a relation, $G(\mathrm{MPa}) = -47 \times T(\mathrm{K}) + 103572)$.[8,9]
37) S. Takeuchi and A. S. Argon: J. Mater. Sci. **11** (1976) 1542–1566.